Experimental and modeling analysis based on Gassmann and Differential Effective Media fluid substitution

Rafael R. S. Guerra*[1 2], Marco Ceia[1], Roseane Missagia[1], Lucas C. Oliveira[1 2], Simonária Fidélis[1 2], Irineu Lima Neto[2],
[1]UENF/LENEP, [2]FACC

This paper was prepared for presentation during the 17th International Congress of the Brazilian Geophysical Society held in Rio de Janeiro, Brazil, 16-19 August 2021.

Abstract

The characterization of fluid-saturated rocks still presents great challenges for the seismic and petrophysical analysis. For these interpretations, the Gassmann fluid substitution and Differential Effective Media (DEM) modeling are widely used. In order to characterize these rocks, this work proposes an integrated study with experimental and modeling parts to evaluate the P and S wave velocities based on Gassmann and DEM models. The experimental workflow was performed with the sample in dry condition, saturated with brine and saturated with oil to determine the P and S waves transit travel times. The Gassmann fluid substitution used as a basis the measured data of the sample and digital image analysis (DIA) was used to estimate the microporosity aspect ratio for DEM modeling. The results for Gassmann fluid substitution were consistent and showed a good correlation with the measured data. Despite the limitations of image resolution of the thin-sections used, the difference between image and gas porosity provided a reasonable estimate of microporosity occurrence in DEM modeling, resulting in good velocities predictions.

Introduction

In rock physics analysis of logs, cores, and seismic data, the characterization of rocks saturated by fluids is yet a complicated subject. Fluid replacement is one of the most commonly used resources to assist the analysis of these rocks, mainly using Gassmann (1951) relationships. Despite the basic assumptions for its calculations, this approach is quite general and robust, and it still provides good results for a wide range of problems. Another difficult task in the analysis is estimating the effective elastic moduli of a rock in terms of its constituents and pore space. One of the methods often used to estimate such parameters is the Differential Effective Media Model (DEM), which models biphasic compounds by incrementally adding inclusions from one phase to the matrix phase (Mavko *et al*., 2020).

The experimental part of this work includes experiments with dry rocks, saturated rocks, and fluid replacement using an adaptation of the Rock Physics System (SFR) installed at LENEP (Lima Neto et al., 2014). This adaptation allows the evaluation of pore pressure (PP) and saturation by fluid injection in the triaxial system, making possible the computation of P and S velocities under different pressure and saturation regimes. The second part of the research consists in simulating fluid substitution using Gassmann and DEM approaches. The fluid replacement simulation was performed initially with the dry rock and substitutions for water and oil, and, later, with the sample saturated in water (brine) with oil substitution. The aim of DEM modeling is to estimate the elastic properties of a sample by taking into account the pore geometry of the material. This modeling was done for dry, brine-saturated, and oil-saturated rock.

Method

Data acquisition

First, we characterize the petrophysical properties of the core plug sample, and then it was carried out by the direct wave transmission test (ASTM D2845-08, 2008) to determine the P and S waves transit travel times. The transmission test is performed in Rock Physics Triaxial System equipment with a Berea sandstone outcrop sample, from the Bedford formation (Ohio – USA), in dry, saturated (brine) and fluid injection (oil) conditions. The properties of the sample are shown in Table 1.

Table 1 *- Physical, petrophysical and mineralogical properties of the Berea standard sample.*

Sample	Berea
Diameter (cm)	7.050
Length (cm)	3.805
Volume (cm^3)	80.170
Gas porosity $(\%)$	20.140
Dry sample density(g/cm^3)	2.113
Grain density (g/cm^3)	2.649
Sample mass in dry condition (g)	169.365
Pore volume (g)	16.227

The experimental workflow consists of some steps. The first step was performed with the sample in dry condition using a triaxial deformation system under a confinement pressure range from 5 to 40 MPa. The register of wave travel time occurred during the load and unload confinement pressure. In the second step, the sample was saturated with brine of 56000 ppm NaCl concentration and the experimental setup was the same as used in the first step.

After that, in the third step, we used a fluid injection system coupled to the triaxial system equipment and performed the oil injection process in the core plug sample. This test considered using the sample previously saturated with brine (56000 ppm) to minimize the rock-fluid interactions because the Berea sample is moderately water-wet (COSTA et al., 2019), thus making the displacement of water through oil more efficient. This step was started with the gradually loading confinement

pressure until the 40 MPa level. When arriving at 40 MPa pressure level, it was started the oil injection process. The oil used is a mixture of diesel fuel and lube oil, with a proportion of 2:1 (two parts of diesel fuel to one of lube oil), and its properties are contents in Table 2. When arriving at 40 MPa pressure level, it was started the oil injection process at a flow of 0.5 ml/min. This procedure resulted in an effluent that was collected at graduated cylinders to quantify the fluid volumes inside the sample (Figure 1).

Table 2 *- General properties of the oil mixture.*

Fluid	Oil Mixture
Composition	2 parts of diesel oil + 1 part of lubricating oil
Mixture Density (g/cm^3)	0.896
°API	26.360
Viscosity	13.830
P wave Velocity (m/s)	1414.230

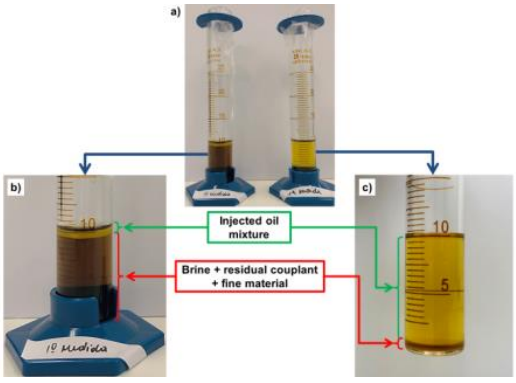

Figure 1 *- Effluent from the injection test composed of a mixture of oil and brine: (a) beakers with the effluent collected in the test; (b) maximization of the region containing the brine phase with fine material, residual coupling and oil; (c) maximization of the beaker containing mostly oil and a thin layer of brine at the bottom.*

Gassmann fluid substitution and DEM modeling

Gassmann's relations uses seismic velocities in rocks saturated with one fluid to predict those of rocks saturated with a second fluid, or equivalently, predicting saturated-rock velocities from dry-rock velocities (Mavko et al., 2020). In this methodology, the shear ($\mu_{sat,1}$) and bulk modulus ($k_{sat,1}$) are calculated for the situation where the rock is saturated with one fluid, in other words, from the measured compressional ($V_{p,1}$) and shear ($V_{s,1}$) wave velocities. The density (ρ) follows Equation 3, where ϕ is the porosity, ρ_{fl} is the fluid density and ρ_s is the solid density.

$$\mu_{sat,1} = \rho . {V_{s,1}}^2 \quad (1)$$

$$k_{sat,1} = \rho . {V_{p,1}}^2 - \frac{4}{3}\mu \quad (2)$$

$$\rho = (1-\phi)\rho_s + \phi . \rho_{fl} \quad (3)$$

As a result, it is possible to perform a fluid replacement and obtain modeled elastic modules for oil-saturated rock condition using the conditions of dry or brine-saturated as data. The Equations 4 - 5 shows the determination of the effective bulk modulus of the rock with pore fluid 2 ($k_{sat,2}$), where k_{dry} is the effective bulk modulus of the drained rock, $k_{fl,1}$ and $k_{fl,2}$ are the bulk modulus of the pore fluid 1 and 2 respectively, and k_s is the bulk modulus of the solid rock component.

$$k_{sat,2} = k_{dry} + \frac{\left(1 - \frac{k_{dry}}{k_s}\right)^2}{\frac{\phi}{k_{fl,2}} + \frac{1-\phi}{k_s} - \frac{k_{dry}}{{k_s}^2}} \quad (4)$$

$$k_{dry} = \frac{k_{sat,1}.(1-\phi) + k_{sat,1}.\frac{k_s}{k_{fl,1}}.\phi - k_s}{\frac{k_{sat,1}}{k_s} + \frac{k_s}{k_{fl,1}}.\phi - (1+\phi)} \quad (5)$$

Once the P and S wave velocities are affected by the presence of the new fluid (Schön, 2011), their values are recalculated based on the modeled modules.

The DEM theory is based on the assumption that the material includes isolated pores, and it models two-phase composites by introducing inclusions of one phase to the matrix phase incrementally until the desired proportion of the constituents is reached (Berryman, 1992):

$$(1-\phi)\frac{d[K^*(\phi)]}{d\phi} = (K_2 - K^*)P^{(*2)}(\phi) \quad (6)$$

$$(1-\phi)\frac{d[\mu^*(\phi)]}{d\phi} = (\mu_2 - \mu^*)Q^{(*2)}(\phi) \quad (7)$$

with the initial conditions $K^*(0) = K_1$ and $\mu^*(0) = \mu_1$, where K_1 and μ_1 are the bulk and shear modulus of the host material, respectively. K_2 and μ_2 are the bulk and shear modulus of the inclusions, respectively, with $K_2 \cong 0$ and $\mu_2 = 0$ for a dry rock. The coefficients $P^{(*2)}$ and $Q^{(*2)}$ are the geometric factors (for detailed expressions of these coefficients, see Berryman, 1980; Mavko et al., 2020) that depend on the aspect ratio of the inclusions.

This modeling is iterative, taking into account the pore geometry of the material at each inclusion until the effective medium is established for the estimation of the elastic modulus of the rock. The pore geometry of the material is characterized by the aspect ratio, which can be obtained through a link between the DEM theory and digital image analysis of thin-sections images from the samples. This technique also allows the estimation of the porosity of the rock and is made from a cross-section in the sample that is impregnated with blue epoxy.

The software used for image analysis was IrfanView and ImageJ in the Fiji version. In IrfanView, the images were converted to 8 bits using the color palette that was developed by Grove and Jerram (2011) and saved as PGN file format. In ImageJ, the jPOR plugin (Grove and Jerram, 2011) was used for image segmentation and porosity analysis. Figure 2 shows a flowchart of the DIA procedures.

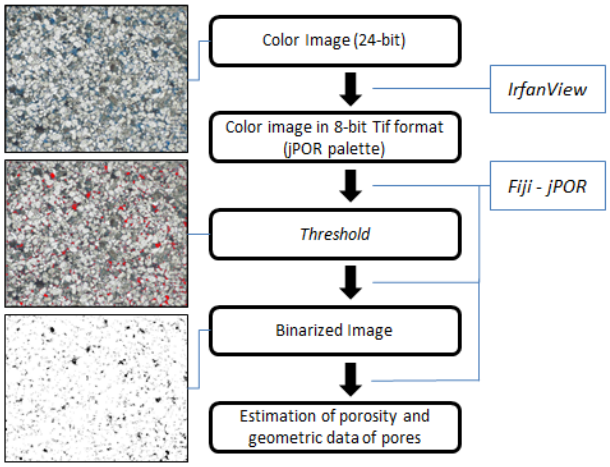

Figure 2 *- Flowchart of petrographic analysis of images with a focus on pore geometry.*

To use the DEM model, it is necessary to estimate the microporosity (ϕ_{micro}), which can be determined through Equation 8. Gas porosity (ϕ_{gas}) can be measured in the laboratory, representing total porosity, that is, it represents all pore scales (macro-meso and micro). The porosity of the image (ϕ_{image}) is found through the slide analysis method, representing only the macro-mesopores. The difference between these two parameters results in microporosity.

$$\phi_{micro} = \phi_{gas} - \phi_{image} \quad (8)$$

The methodology for estimating the microporosity aspect ratio follows the model established by Lima Neto *et al*. (2014) to predict the microporosity inclusion aspect ratio, characterize pore geometry parameters and complexities related to the elastic properties of rocks.

Results

The Gassmann model uses as input the parameters obtained from the rock, fluids and the waves velocities measured in dry and saturated (brine) conditions. As a result, it was possible to determine the values of P and S wave velocities through fluid substitutions: air for water, air for oil and water for oil. The results are show in Table 3.

Table 3 *- Velocities obtained by Gassmann fluid substitution for the cases: air-water, air-oil and water-oil.*

	Gassmann air-water		Gassmann air-oil		Gassmann water-oil	
Pressure	V_p	V_s	V_p	V_s	V_p	V_s
5	3.45	1.91	3.40	1.92	3.43	2.03
10	3.73	2.13	3.69	2.14	3.72	2.16
15	3.82	2.22	3.78	2.23	3.79	2.24
20	3.88	2.27	3.84	2.27	3.87	2.28
25	3.92	2.30	3.89	2.31	3.88	2.31
30	3.94	2.32	3.91	2.33	3.88	2.33
35	3.95	2.34	3.91	2.35	3.92	2.35
40	3.97	2.34	3.93	2.35	3.91	2.36

The behavior of V_p and V_s in dry and oil-saturated conditions with respect to pressure variation is shown in Figure 3. It's possible to observe that as the pressure grows, the velocity rises as well, gradually stabilizing. According to Lima Neto et al. (2014), this behavior occurs because when an effective pressure is applied, there is a reduction in microporosity which leads to an increase on the wave velocity by increasing the predominance of rounded macro-mesopores and reducing the bulk porosity.

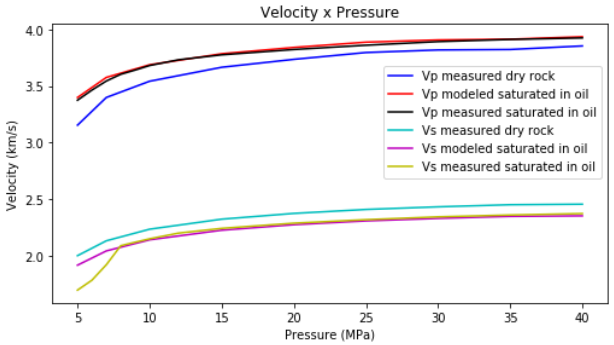

Figure 3 *- Comparison of velocities measured in the laboratory and modeled as a function of pressure for the cases of dry and oil-saturated rock. The modeled velocities were obtained by Gassmann fluid substitution for the case of oil saturation.*

Figure 4 shows a comparison of velocities as a function of effective pressure in the case of rock saturated in water and saturated in oil. It was observed that modeled and measured V_p for the oil-saturated sample were lower than V_p in the water-saturated condition. This behavior was expected because the greater the density of the fluid, the greater the velocity of the P wave.

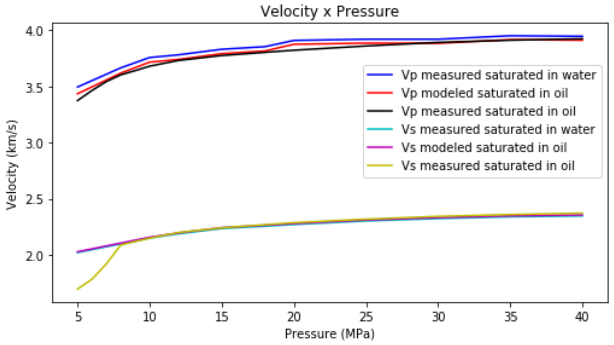

Figure 4 *- Comparison of velocities measured in the laboratory and modeled as a function of pressure for the cases of rock saturated with water and saturated with oil. The modeled velocities were obtained by Gassmann fluid substitution for the case of oil saturation.*

It was possible to calculate the percentage of occurrence of aspect ratio (macro-meso) of the thin sections, as well as their average, using digital image analysis. Figure 5 shows that a ratio of approximately 0.5 occurs 25% of the time in one of the analyzed images.

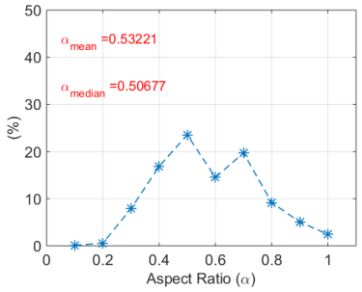

Figure 5 *- Pore Aspect Ratio estimated from a thin section. The graph shows the mean and median values.*

The purpose of DEM modeling is to determine the microporosity's aspect ratio, which combined with the macro-mesopore data (obtained through DIA), petrophysical data and elastic properties, allow characterizing the rock sample. In this methodology (Lima Neto *et*. Al., 2015), the three types of porous system are considered in two inclusion scenarios: 1) macro-meso pore, in which the aspect ratio is established through digital image analysis, and 2) microporous, predicted by the measured P-wave velocity as it reflects pore conditions with good reliability.

With the macro-mesoporous aspect ratio data, it was possible to estimate the microporosity aspect ratio through DEM modeling and the acoustic wave velocities.

Table 4 *- Velocities obtained by DEM modeling for the cases: air, water and oil.*

	DEM air		DEM water		DEM oil	
Pressure	V_p	V_s	V_p	V_s	V_p	V_s
5	3.16	2.14	3.50	2.08	3.38	2.03
10	3.54	2.38	3.76	2.30	3.68	2.28
15	3.67	2.46	3.82	2.35	3.78	2.36
20	3.74	2.50	3.91	2.42	3.83	2.39
25	3.80	2.54	3.91	2.42	3.86	2.42
30	3.82	2.55	3.91	2.42	3.89	2.44
35	3.82	2.55	3.96	2.46	3.92	2.46
40	3.85	2.58	3.94	2.45	3.93	2.47

Figure 6 shows a comparison between modeled velocities (DEM) and measured in the laboratory. In the color bar it is possible to observe the adjustment coefficient (R) obtained through Equation 9 to evaluate the results.

$$R = 1 - \frac{|V_{measured} - V_{DEM}|}{V_{measured}} \quad (9)$$

We can observe in the Figure 6 that there was an excellent adjustment of measured and modeled velocities because the data follow the dotted line (45°) of the graph. The coefficient of determination (R^2) suggested that the data was well-fitting, reaching values close to 1. Another feature observed is an increase in the adjustment coefficient (R) as the confinement pressure rises, which is consistent with the theory that microporosity decreases as pressure is increased (Lima *et al.*, 2015). In particular, the case modeled for oil (Figure 6c) did not reflect the decrease in microporosity because it was an approximation (mixture of oil and brine present in the rock) making the small variation of the coefficient R not to be observed. The same behavior was not observed for V_s, which, despite having an R^2 close to 1 and demonstrating the effect of pressure on microporosity, did not show a good correlation between the measured and modeled data.

Another approach adopted was the use of elastic modules k_{DEM} and μ_{DEM}, obtained through DEM modeling, to estimate the velocities. In this methodology, k_{DEM} was considered as k_{dry} and applied in Equation 4 to determine a new k_{sat}. Subsequently, the P and S wave velocities saturated in water and oil were estimated based on dry rock condition.

The Figures 7 and 8 shows a comparison between the methodologies approached and the data measured in the laboratory. To facilitate visualization, the comparison was made based on two scenarios: 1) oil-saturated rock and; 2) water-saturated rock, both cases initially in dry rock condition.

It was observed in the first scenario that V_p modeled from dry rock presented a better fit to the laboratory data than V_p modeled from water saturated rock, which is why we chose air-oil instead of water-oil modeling for the comparison. In this case, all the methodologies approached presented satisfactory results, with good approximation to the measured data and also a good correlation coefficient, which shows consistency in the method.

It's worth mentioning that the DEM modeling provided the best fit to the measured data for V_p. In the case of V_s, the same did not occur because the best results were achieved by Gassmann substitution. When observing the comparison for Vs, it is noticed that the results for low pressures (5MPa and 7MPa) differed from the general behavior, a fact that is explained due to the low coupling of the sample to the equipment, generating less reliable results. All methods showed good correlation (R^2), which demonstrates the consistency of the approached methodology.

In the second scenario, the DEM modeling again showed a better correlation with the laboratory data for V_p. In this case, the DEM Gassmann modeling was able to better reproduce the behavior of V_p for low pressures when compared to the air-oil case. Analyzing the results for V_s, the DEM modeling and the DEM Gassmann substitution had worse results when compared to the Gassmann method. This characteristic can be attributed to the use of constant porosity in the modeling, making the S wave, which does not propagate in the fluid, not be compensated by the reduction of the porosity with the increase in pressure, which explains the slight difference of about $0.12\ km/s$ observed.

Conclusions

The P and S wave velocities of a sandstone sample with quartz predominance (Berea) were determined using tests conducted in dry, saturated, and with fluid injection conditions. Based on data obtained experimentally, Gassmann's methodologies for fluid substitution and DEM modeling were used in order to estimate the velocity in conditions of water and oil saturated rock.

The results for fluid substitution were consistent and showed a good correlation with the measured data. Despite the limitations of image resolution, the difference between image and gas porosity provided a reasonable estimate of microporosity occurrence in DEM modeling, resulting in good velocities predictions. Another weak point identified was the use of porosity as a constant in the modeling due to equipment limitations, which resulted in a slight variance in the prediction of shear wave velocity. In addition, a new approach was proposed considering k_{DEM} of the DEM modeling as k_{dry} of the Gassmann Equation to estimate the velocities. This approach showed satisfactory results, with better adjustment in the compressional wave velocity estimation.

Acknowledgments

Authors thank UENF/LENEP for all structure provided to the execution of this work. This study was financed in part by the Coordenação de Aperfeiçoamento de Pessoal de Nível Superior - Brasil (CAPES) - Finance Code 001 and part by Petrobras (Process 2017/00067-9). MC and RM thank INCT/Geofisica for financial support; and also, CNPq for their Research Grants of Productivity in Technological Development and Innovation – DT II. We are also grateful to Remilson Rosa for helping during the experiments.

References

ASTM D2845-08, 2008. Standard Test Method for Laboratory Determination of Pulse Velocities and Ultrasonic Elastic Constants of Rock (Withdrawn 2017). ASTM Int.

BERRYMAN, J. G., 1992. Single-scattering approximations for coefficients in Biot's equations of poroelasticity. The Journal of the Acoustical Society of America, v. 91, p. 551–571. DOI: http://dx.doi.org/10.1121/1.402518.

Costa, V., Missagia, R., Ceia, M., 2019. Wettability Measurement and Its Impact in Converted Capillary Pressure Curves. 16th International Congress of the Brazilian Geophysical Society, Rio de Janeiro, Brazil.

GROVE C., JERRAM D. A., 2011. jPor: An ImageJ macro to quantify total optical porosity from blue-stained thin sections. Computers & Geosciences. 1850-1859.DOI: https://doi.org/10.1016/j.cageo.2011.03.002.

LIMA NETO, I.; MISSÁGIA, R. M; CEIA, M. R.; ARCHILHA, N. L.; HOLLIS, C., 2015. Evaluation of carbonate pore system under texture control for prediction of microporosity aspect ratio and shear wave velocity. Sedimentary Geology 323. Elsevier, pp. 43-65. DOI: https://doi.org/10.1016/j.sedgeo.2015.04.011.

LIMA NETO, I.A., Misságia, R.M., Ceia, M.A., Archilha, N.L., Oliveira, L.C., 2014. Carbonate pore system evaluation using the velocity–porosity–pressure relationship, digital image analysis, and differential effective e medium theory. Journal of Applied Geophysics 110. Elsevier, pp.23–33. DOI: http://dx.doi.org/10.1016/j.jappgeo.2014.08.013.

MAVKO, G., T. MUKERJI, AND J. DVORKIN, 2020. The rock physics handbook: Tools for seismic analysis of porous media: Cambridge university press.3rd Edition.

SCHÖN, J. H., 2011. Physical Properties of Rocks: a workbook. Amsterdam: Elsevier, 481p.

SMITH, T.M., SONDERGELD, C.H., RAI, C.S., 2003. Gassmann fluid substitutions: a tutorial. Geophysics 68, 430-440.

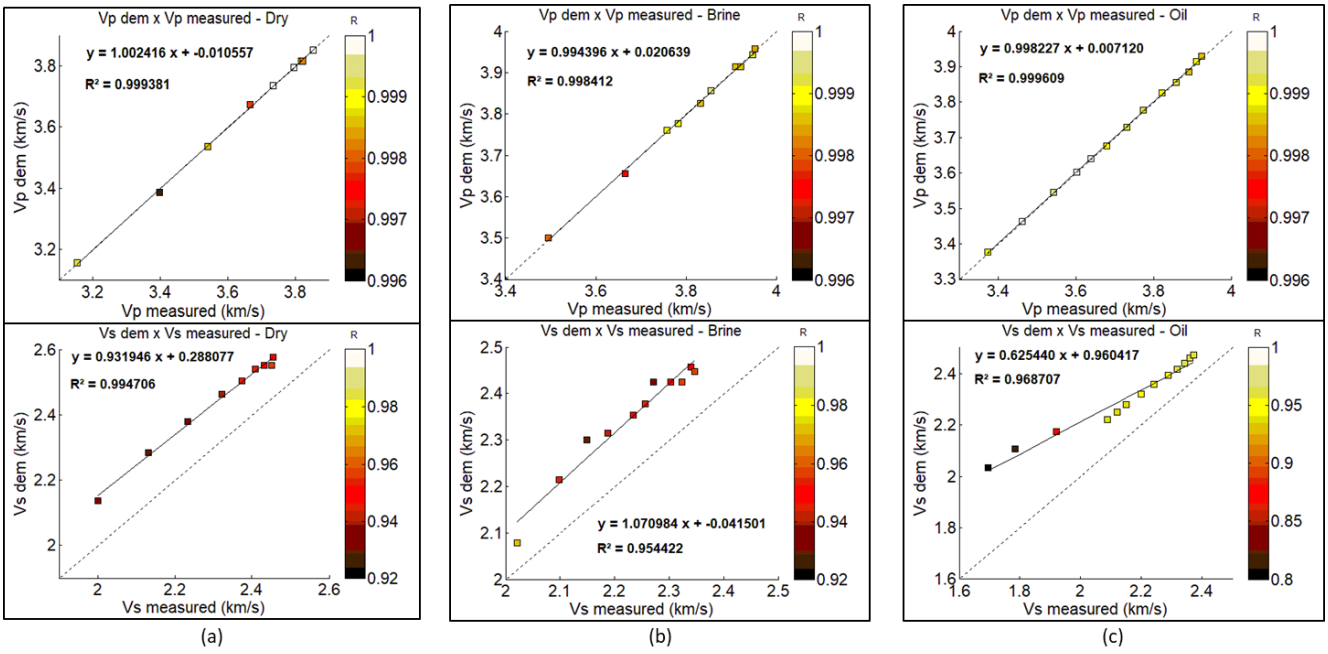

Figure 6 *- Comparative graph of P and S wave velocities determined by acoustic measurements and estimated by DEM modeling with their respective exponential adjustments R² and coefficient of determination R for the cases: (a) Dry rock; (b) Brine-saturated rock; and (c) Oil-saturated rock.*

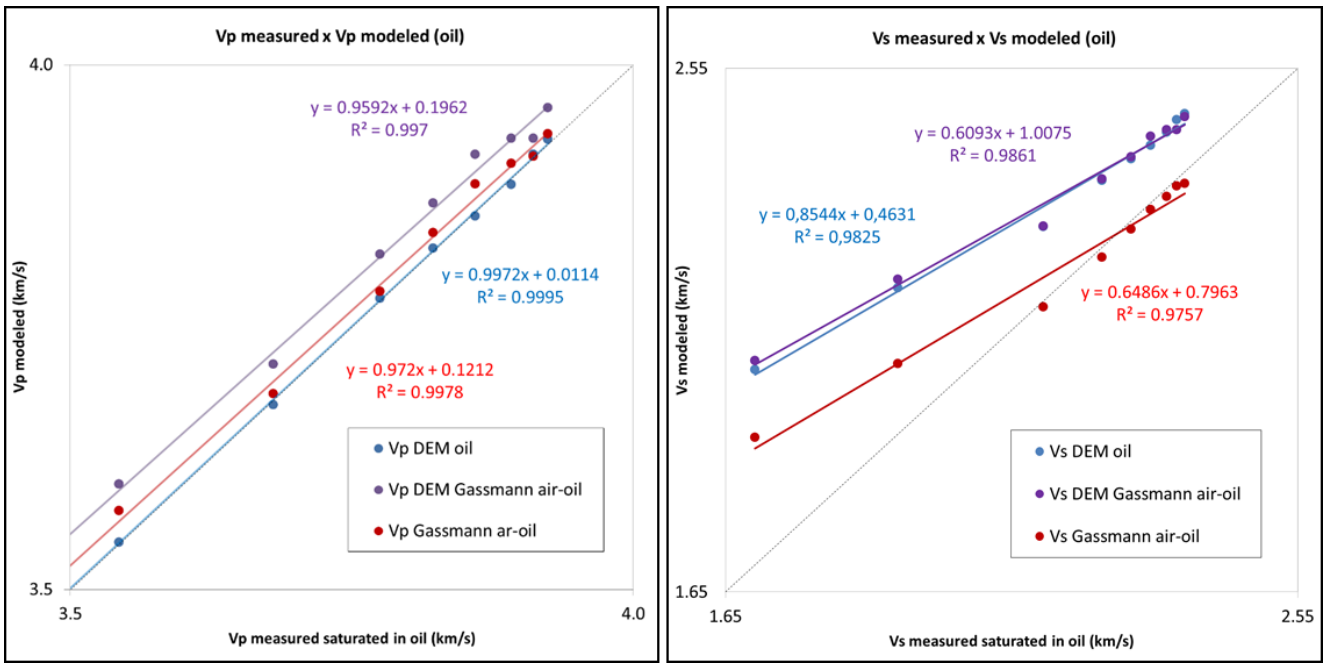

Figure 7 *- Graph of V_p and V_s measured in laboratory with the sample saturated in oil (S_w = 0.38 and S_o = 0.62) versus V_p and V_s modeled by the methods: DEM (blue); Gassmann (red); and DEM-Gassmann, with DEM modeling performed in dry rock conditions to obtain k_{DEM} and perform the air-oil substitution by Gassmann where $k_{dry} = k_{DEM}$ (purple).*

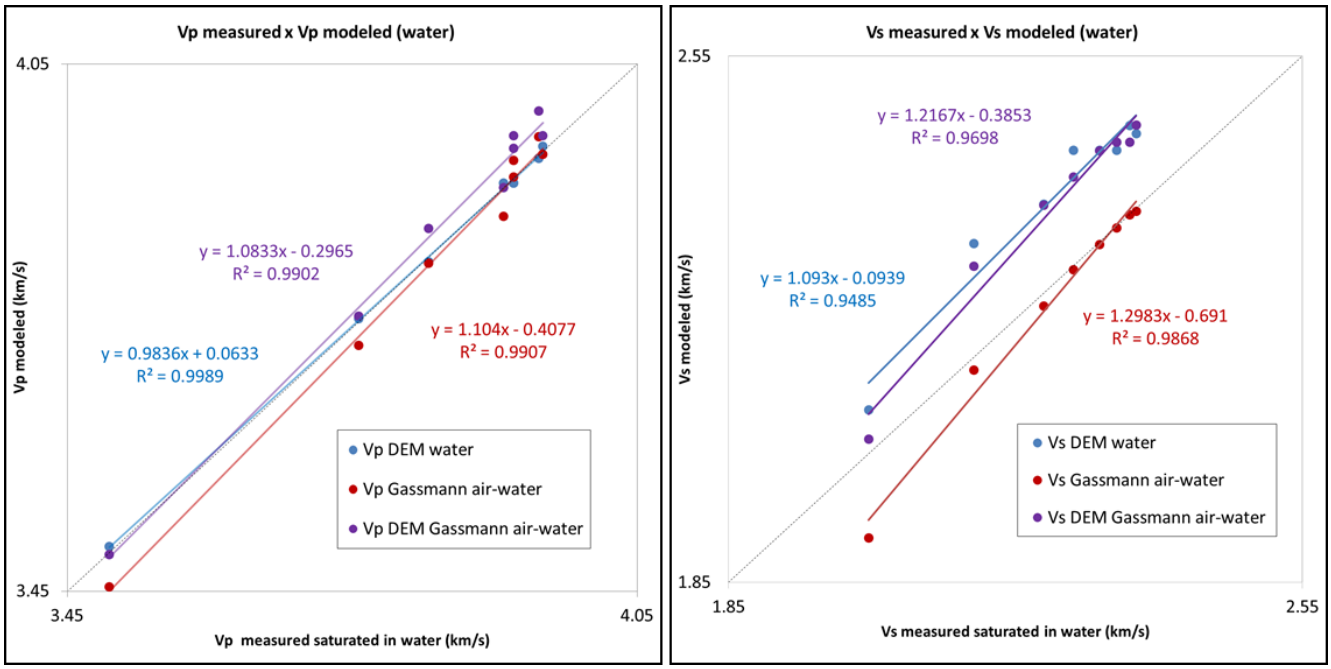

Figure 8 *- Graph of V_p and V_s measured in laboratory with the sample saturated in water (brine $S_w \cong 1$) versus V_p and V_s modeled by the methods: DEM (blue); Gassmann (red); and DEM-Gassmann, with DEM modeling performed in dry rock conditions to obtain k_{DEM} and perform the air-water substitution by Gassmann where $k_{dry} = k_{DEM}$ (purple).*